SAND2016-1333C

A METHOD FOR EXTRAPOLATING HAVERSINE SHOCK TEST INPUT LEVELS

Carl Sisemore, Troy Skousen
Sandia National Laboratories*
Albuquerque, NM 87185

ABSTRACT

Fitting a haversine shock response spectrum to field collected shock data is an accepted method for subsequently performing laboratory tests or numerical system level analyses. However, in a situation where a system is required to demonstrate performance at one level but asked to simulate or evaluate performance at another, higher level, it is often uncertain how to extrapolate the shock response to different severities. To perform this analysis, an understanding of how the shock response spectrum is changed from one input level to another is necessary. In this example, a single system level drop shock test was performed in the field. A haversine shock response spectrum was fit to the experimental data for use in evaluating the system and sub-components. Since no further system level testing was conducted, an analytical methodology for extrapolating the resulting shock input was required for evaluation of the system at different drop heights. An analytical method for extrapolating the shock response spectrum of a system sub-component was developed using the conservation of energy relationships for a system in free-fall. This resulted in a shock response spectrum extrapolation technique based on a combined scaling of the input velocity and shock period. Subsequent laboratory testing of a similar instrumented system at several different shock input levels was compared against the extrapolation method to evaluate the proposed scaling methodology.

INTRODUCTION

Shock data collected in the field is frequently simplified for subsequent laboratory testing on standard test machines. Testing can be performed on drop tables, resonant fixtures, electrodynamic or hydraulic shakers, or other machines. One example of this simplification is the fitting of a haversine shock response spectrum (SRS) to field collected data for use on a drop table. The haversine shock can then be easily reproduced in the laboratory. However, it is often desired to test equipment to levels other than those tested in the field. Interpolating levels between two or more field tests is relatively straightforward; however, it is often desirable to extrapolate testing beyond the levels tested in the field. Worse yet is the situation where only one field test was performed and the need arises to extrapolate that test to a level far beyond the as-tested level.

Drop tables typically produce a haversine shock and are representative of shocks resulting from a rapid velocity change. An example of this is a scenario in which a component is dropped from some arbitrary height, either purposefully or accidentally, onto a relatively hard surface. In this scenario, the three primary factors are the free height of the fall, the impacting surface composition, and the structure of the component itself. There are many benefits to drop table testing: high shocks can be obtained over short durations similar to a free-fall onto a hard surface; laboratory testing is relatively quick and economical; tests are very repeatable; drop table tests are representative of many real-life environments; and the drop table shock profile is easily represented mathematically.

In contrast to a free-fall drop, haversine shock pulses are typically defined in terms of acceleration magnitude, pulse duration, and the damping coefficient. Scaling of the shock pulse should appropriately scale one or more of these parameters. The first step in determining how a shock pulse should be scaled is to determine the parameters of the shock pulse from the field test. To this end a method for optimized curve fitting of experimental data with a haversine SRS is presented. Once a haversine is fit to the data, a methodology for scaling the SRS to the desired level is needed. A scaling approached based on conservation of energy methods is derived and presented. Finally, data from a representative test series are presented to validate the analytical work presented here.

* Sandia National Laboratories is a multi-program laboratory managed and operated by Sandia Corporation, a wholly owned subsidiary of Lockheed Martin Corporation, for the U.S. Department of Energy's National Nuclear Security Administration under contract DE-AC04-94AL85000.

HAVERSINE CURVE FITTING

Fitting test data to an idealized function can be a somewhat subjective endeavor. It can also be time consuming. Curve fitting methods have been available in numerous forms for almost as long as computers have been used for data processing. A simple approach for data fitting is presented here which makes use of the downhill simplex method of Nelder and Mead [1]. To implement this method, an SRS from an ideal haversine shock is calculated using choices for amplitude, pulse duration, and damping. This idealized SRS is then compared to the SRS calculated from an accelerometer test record. The difference between the two curves is computed and converted to a single scalar value measuring the goodness of the fit. Subsequent iterations of the simplex optimizer use different values for amplitude, pulse duration, and damping to minimize the error function between the idealized SRS and the SRS of the test data. An example of one such curve fit is shown in Figure 1. Here the simplex optimizer seeks to minimize the difference between the test data SRS and the idealized haversine SRS. As a result the idealized curve tends to fare through the test data resulting in a reasonably good representation of the as-tested environment.

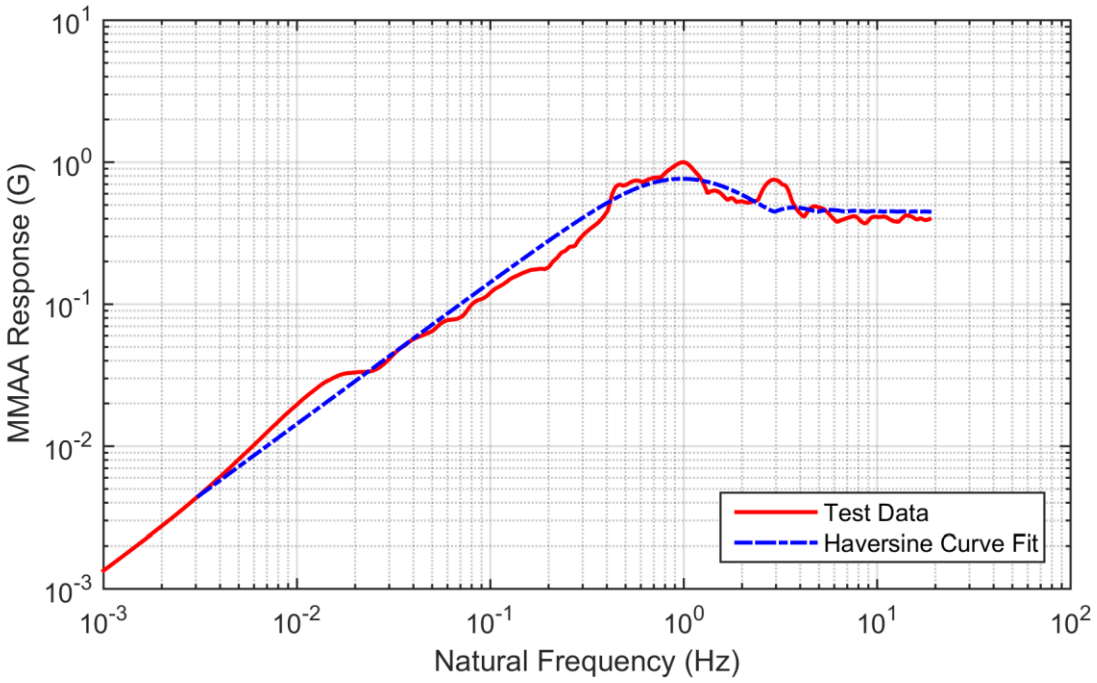

Figure 1. Sample Haversine Curve Fit to Normalized Test Data Using Function Minimization Technique

One additional benefit of this method is that regions of obviously corrupt data can be excluded from consideration in the goodness-of-fit algorithm. For example, in Figure 1, it is obvious that an additional frequency component is present in the data in the 3Hz region which is not part of the actual haversine input. Therefore, the scalar valued function can be tailored to exclude that bump in the SRS from consideration during the fitting operation.

This method for fitting test data using a Nelder-Mead simplex optimizer is used throughout this paper to ensure consistency in the interpretation of the data.

ENERGY SCALING METHODOLOGY

The method starts out by assuming that at least one field drop test has been performed on the component of interest. Without any field data there would be no resulting test specifications to scale or extrapolate. The scaling

methodology presented here is based on conservation of energy. Conservation of energy relations always begin with an estimate of the energy in the system. For the case of an object under free fall, the energy in the system is very simply given by the mass of the system and the drop height. The potential energy is simply:

$$U_h = mgh. \tag{1}$$

The kinetic energy is likewise given by:

$$T = \frac{1}{2}mv^2. \tag{2}$$

Thus, it is obvious and well known that the impact velocity is independent of the component mass and is given by:

$$v = \sqrt{2gh}. \tag{3}$$

Thus, a 10ft free fall results in an impact velocity of 25.4ft/sec and a 20ft free fall results in a 35.9ft/sec impact velocity for example. The energy is linearly proportional to drop height as shown in Equation (1) and the velocity is a function of the square root of drop height as shown in Equation (3).

Thus, a 20ft drop height contains double the energy of a 10ft drop height but the impact velocity is only 141 percent greater. The question then is how to appropriately represent all of the impact energy in the system? It is also readily intuitive that a higher drop height should result in greater compression of the impacting components. Dropping a part from a greater height typically results in more damage. This can be expressed by considering the stiffness and deformation of the component under test. Thus, from the conservation of energy relations, the potential energy stored in a spring is given by:

$$U_s = \frac{1}{2}ky^2. \tag{4}$$

Here the displacement term, y, would be a combination of the deflection of both the falling components and the impact surface and the spring rate, k, is a combination of the component stiffness and the stiffness of the impact surface. Since energy must be conserved, the potential energy prior to the drop, U_h, must be equal to the kinetic energy immediately prior to impact, T, which in turn must be equal to the maximum energy stored in the spring system when the velocity is zero at the maximum impact depth, U_s. Thus:

$$mgh = \frac{1}{2}ky^2. \tag{5}$$

Rearranging and solving for y gives:

$$y = \sqrt{\frac{2mgh}{k}} = \sqrt{2gh}\sqrt{\frac{m}{k}} = \frac{\sqrt{2g}}{\omega}\sqrt{h}. \tag{6}$$

Equation (6) makes the familiar substitution for the system natural frequency and shows that the impact depth is a function of frequency and the square root of the drop height. As expected then, the impact depth for the 20ft drop height will be greater than for the 10ft drop height by a factor of 141 percent. For greater impact depths, the impact time will of necessity be proportionately longer. Displacement is naturally given as a function of acceleration and impact velocity by the well-known relation:

$$y = y_0 + v_0 t + \frac{1}{2}at^2. \tag{7}$$

For a traditional haversine shock, the velocity change is a function of the pulse duration and the maximum acceleration as:

$$v_0 = \frac{1}{2}at. \tag{8}$$

Substituting Equation (8) into Equation (7) and making the assumption that $y_0 = 0$ yields:

$$y = at^2. \tag{9}$$

Thus, the impact depth is also a function of time squared or reversing this expression, the impact time is proportional to the square root of impact depth or the fourth-root of the drop height. For the example above then, the drop height is doubled which results in a factor of $\sqrt{2} = 1.41$ increase in impact velocity and a factor of $\sqrt[4]{2} = 1.189$ in the pulse width. This is shown graphically in Figure 2 for a theoretical doubling of the drop height from the shock data shown in Figure 1. In Figure 2 it can be readily seen that the SRS moves up in magnitude and the peak moves down in frequency.

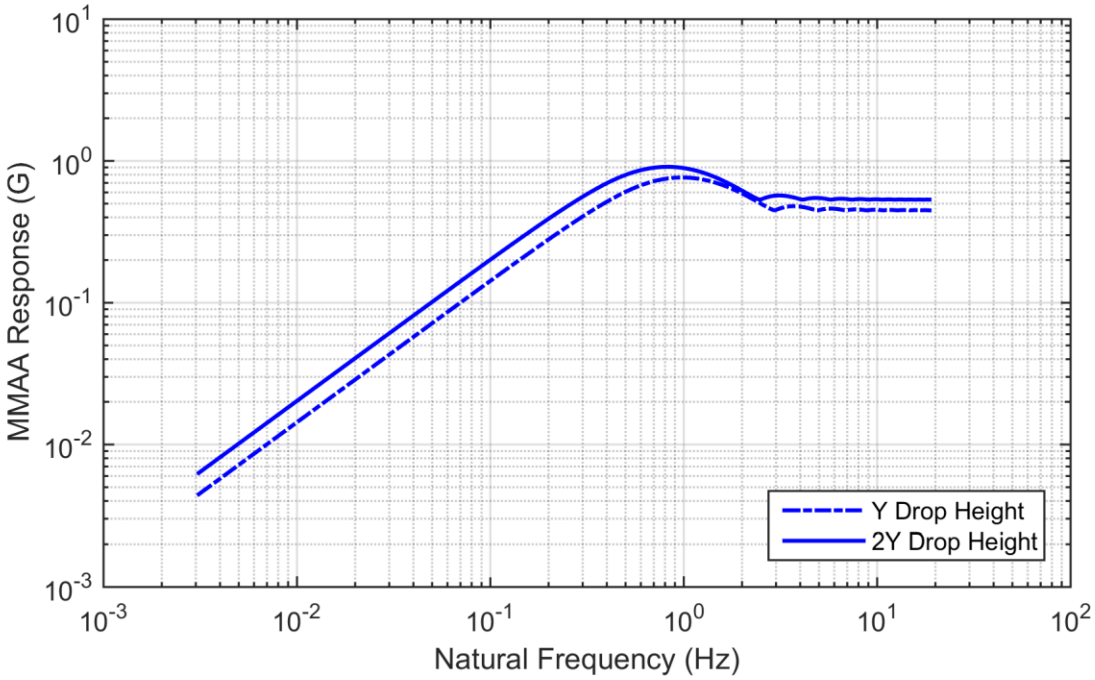

Figure 2. Scaling of Previously Calculated Haversine Shock for Drop Height Doubling

The above derivation results in scaling for the velocity and pulse duration for a haversine shock; however, haversine shocks are typically defined in terms of a pulse duration and a peak acceleration. The relationship between peak acceleration and velocity change is straightforward and given in Equation (8). In terms of a ratio between two haversine shocks, the constant multiplier in Equation (8) cancels, and the expression is reduced to:

$$\frac{v_2}{v_1} = \frac{a_2}{a_1}\frac{t_2}{t_1}. \tag{10}$$

Since the ratio of velocities is a function of the square root of the drop height ratio and the ratio of the pulse duration is a function of the fourth-root of the drop height ratio, the peak acceleration ratio should also be a function of the fourth-root of the drop height ratio.

The previous derivation holds if the impact surface is unchanged. However, in the laboratory, it is relatively easy to adjust drop table settings and as a result the pulse duration can be changed to suite or even held nearly constant as drop height increases. In the event that the pulse durations are not allowed to respond naturally an adjustment to the peak acceleration is required. In the special case where the pulse durations are held constant, or nearly constant, the ratio of peak accelerations becomes approximately equal to the velocity ratio or the square root of the drop height. This is relatively easy to accomplish on a drop table but not typical in a field test. Since the pulse durations are typically available from the collected data, it is possible to derive an expression for the ratio of peak acceleration as simply:

$$\frac{v_2/v_1}{t_2/t_1} = \frac{\sqrt{\Delta h}}{t_2/t_1} = \frac{a_2}{a_1}. \tag{11}$$

In the special case where $t_1 = t_2$, the acceleration magnitude ratio equals the velocity change ratio. Therefore, the following scale factors can be used for adjusting a derived haversine shock:

$$\begin{aligned} \frac{v_2}{v_1} &= \Delta v = \sqrt{\Delta h} \\ \frac{t_2}{t_1} &= \Delta t = \sqrt[4]{\Delta h} \\ \frac{a_2}{a_1} &= \Delta a = \frac{\Delta v}{\Delta t}. \end{aligned} \tag{12}$$

SHOCK TEST EXAMPLE

Recently, a shock test series was conducted in the laboratory presenting an opportunity to evaluate the derivation presented here. The test item being evaluated was instrumented and tested on a drop table at three different impact heights. Although the drop table used is an accelerated fall drop table it is still possible to make use of the relations developed here. An accelerometer was installed on the drop table carriage during the test and the response from this accelerometer was integrated to determine the velocity immediately prior to impact. From this, it is possible to determine an equivalent free-fall drop height. The drop height ratio between tests one and two was determined to be 1.47 and the drop height ratio between tests one and three was determined to be 2.48. The drop height ratio between the three tests are listed in Table 1. Since the previous derivation is always in terms of a ratio, the experimental data was normalized to the lowest level drop test. Given the drop height ratio, it is possible to compare the relationship between the haversine amplitude and pulse duration at the component levels.

Table 1. Shock Test Drop Height Ratios and Scale Factors

Shock Test	Drop Height Ratio, h	$\sqrt{h}$	$\sqrt[4]{h}$
1	1.000	–	–
2	1.469	1.212	1.101
3	2.482	1.576	1.255

One complicating factor with the series of tests used for this analysis is that the impacting surface was altered between shots to maintain a relatively constant pulse duration. As discussed previously, as the drop height and impact velocity increase, the impact time should also increase proportionately. However, in this case the impact times actually decreased slightly with each successive shot as a result of alterations to the impact surface. Therefore, the haversine peak acceleration is scaled as discussed previously. The haversine peak acceleration factors for these particular tests are listed in Table 2.

Table 2. Haversine Peak Acceleration Amplitude Scale Factors

Shock Test	Drop Height Ratio, h	Pulse Duration Ratio	Acceleration Factor
1	1.000	–	–
2	1.469	0.986	1.228
3	2.482	0.957	1.647

Three internal components were instrumented during these tests, labeled component A, B, and C. There were three accelerometers located on component A, labeled A-1, A-2, and A-3; two accelerometers on component B, labeled B-1 and B-2; and a single accelerometer on component C. The first step in the evaluation process was to use the Nelder-Mead method to fit a haversine SRS to all of the shock data collected at the various components. The data was subsequently normalized to the maximum acceleration and pulse duration at the fixture base from the first shock test. This normalized data is presented in Table 3. As expected, components A and B experienced similar but slightly reduced peak acceleration levels compared to the fixture base. This is a result of the test fixture and component frame acting as a filter for the shock energy. Components A and B were also similar in size and mounting configuration. Component C experienced a substantial amplification of the acceleration level during both shock events. This is due to the fact that component C has a substantially different size and mounting arrangement than the other two components. The second shock test was performed at a significantly higher amplitude, nearly a third higher, with approximately the same pulse duration at the fixture base. As expected, Table 3 shows that the normalized peak acceleration and the normalized pulse duration increased for all components. Table 4 summarizes the component acceleration and pulse duration ratios between tests one and two and compares the average ratio to the predicted ratio from Table 1 and Table 2. As can be seen, the percent error between the theory and the test averages are well within the expected experimental uncertainty.

Table 3. Normalized Shock Amplitude and Pulse Duration from Test 1 and 2

Component and Location	Shock Test #1		Shock Test #2	
	Normalized Acceleration A_1 (g)	Normalized Pulse Duration t_1 (msec)	Normalized Acceleration A_2 (g)	Normalized Pulse Duration t_2 (msec)
Fixture Base	1.000	1.000	1.3055	0.9863
A-1	0.9678	0.9776	1.1089	1.0682
A-2	0.9202	0.9580	1.1082	1.0442
A-3	0.8522	0.9614	1.0310	1.0493
B-1	0.9121	1.0247	1.0669	1.1055
B-2	0.8493	1.0210	1.0454	1.1133
C	1.8264	0.4690	2.1695	0.4971

Table 4. Comparison of Shock Amplitude and Pulse Duration Ratios, Test 2 to Test 1

Component and Location	A_2/A_1	t_2/t_1
A-1	1.1458	1.0927
A-2	1.2043	1.0899
A-3	1.2097	1.0914
B-1	1.1696	1.0789
B-2	1.2309	1.0905
C	1.1878	1.0601
Component Average	**1.191**	**1.084**
Theoretical Value	**1.229**	**1.101**
Percent Error	**3.04%**	**1.54%**

Figure 3 shows test data SRS result for two gages comparing test one responses to test two responses along with the test two prediction from the theory developed here. As predicted, the haversine SRS profile clearly increases in magnitude and the haversine frequency decreases in frequency and the test two results are very close to the theoretically predicted results.

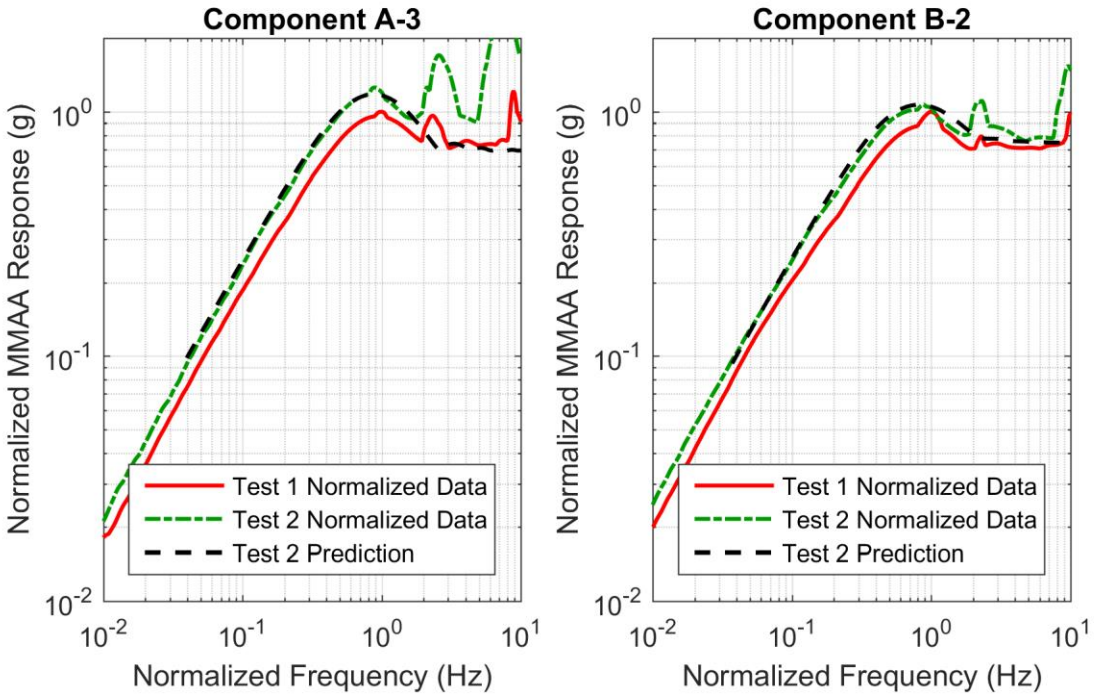

Figure 3. Sample Normalized Data from Test 1 and 2 Showing Shock Pulse SRS Shifting Up in Amplitude and Down in Frequency Along with Test 2 Prediction from Theory

Test 3 is interesting since half of the attachment points failed during the test. As a result, the stiffness was significantly altered during the test and the results are not anticipated to match with the theory; however, the comparison is useful. In addition to the attachment point failures, the gage on component C also failed during the test so no comparison with that component is possible.

Here again, the Nelder-Mead method of fitting a haversine SRS to the shock data was used. The data was then normalized to the fixture base maximum acceleration and pulse duration from the test one. The normalized data for tests two and three are presented in Table 5. Test three was performed at a significantly higher amplitude than test two, nearly a third higher, with approximately the same pulse duration at the fixture base. As expected, Table 5 shows that the normalized peak acceleration increases for all components. In contrast, the pulse duration actually decreases for all components in approximately the same proportion as the fixture base pulse duration which decreased slightly between tests two and three.

Table 5. Normalized Shock Amplitude and Pulse Duration from Test 2 and 3

Component and Location	Shock Test #2		Shock Test #3	
	Normalized Acceleration A_1 (g)	Normalized Pulse Duration t_1 (msec)	Normalized Acceleration A_2 (g)	Normalized Pulse Duration t_2 (msec)
Fixture Base	1.3055	0.9863	1.7117	0.9567
A-1	1.1089	1.0682	1.4389	1.0495
A-2	1.1082	1.0442	1.4378	0.9961
A-3	1.0310	1.0493	1.2998	1.0471
B-1	1.0669	1.1055	1.3572	1.0983
B-2	1.0454	1.1133	1.3809	1.0615

Table 6 summarizes the component acceleration and pulse duration ratio between tests two and three and compares the average ratio to the predicted ratio from Table 1 and Table 2. As can be seen here, the measured acceleration ratio matches with the derived theory very well; the percent error is almost as small as for the first two tests. The measured pulse duration ratio; however, is significantly different from the predicted pulse duration. This is related to the failure of the attachment points. Since some of the attachment points failed during the test, the amount of energy stored in the spring is of necessity reduced. Since the pulse duration ratio is related to the energy stored in the spring, it should inherently come up short as is shown here.

Table 6. Comparison of Shock Amplitude and Pulse Duration Ratios, Test 3 to Test 2

Component and Location	A_2/A_1	t_2/t_1
A-1	1.2976	0.9825
A-2	1.2975	0.9539
A-3	1.2607	0.9979
B-1	1.2721	0.9934
B-2	1.3209	0.9535
Component Average	**1.290**	**0.976**
Theoretical Value	**1.340**	**1.140**
Percent Error	**3.77%**	**14.4%**

Figure 4 shows the test data SRS results for the same two gages comparing test one, two, and three SRS responses. As seen from the tabular data, test three shows the expected increase in magnitude but no obvious downward shift in the pulse frequency. The frequency of the test three haversine pulse is almost vertically above the test two haversine pulse whereas the test two pulse is obviously shifted downward compared to test one. Figure 4 also shows the test three prediction derived from the theory developed here. As can be seen the shock magnitude from the actual test and the test prediction are very close; however, the theory predicts a downward shift in frequency which is not seen in the test data. Again indicating a significant alteration in the system stiffness and that the theory breaks down as the structure fails as would be expected.

One could reasonably infer from the previous derivations that given these three curves it might be possible to extrapolate the point of failure between tests two and three. If test three had been close to the failure point then it would be reasonable to assume that some downward shift in the haversine frequency might be evident. On the other hand, since the test three pulse is almost vertically above the test two pulse, it is reasonable to assume that the failure point was closer to the test two level than the test three level. Sufficient data is not available from this test series to elaborate on this theory but further testing could be warranted.

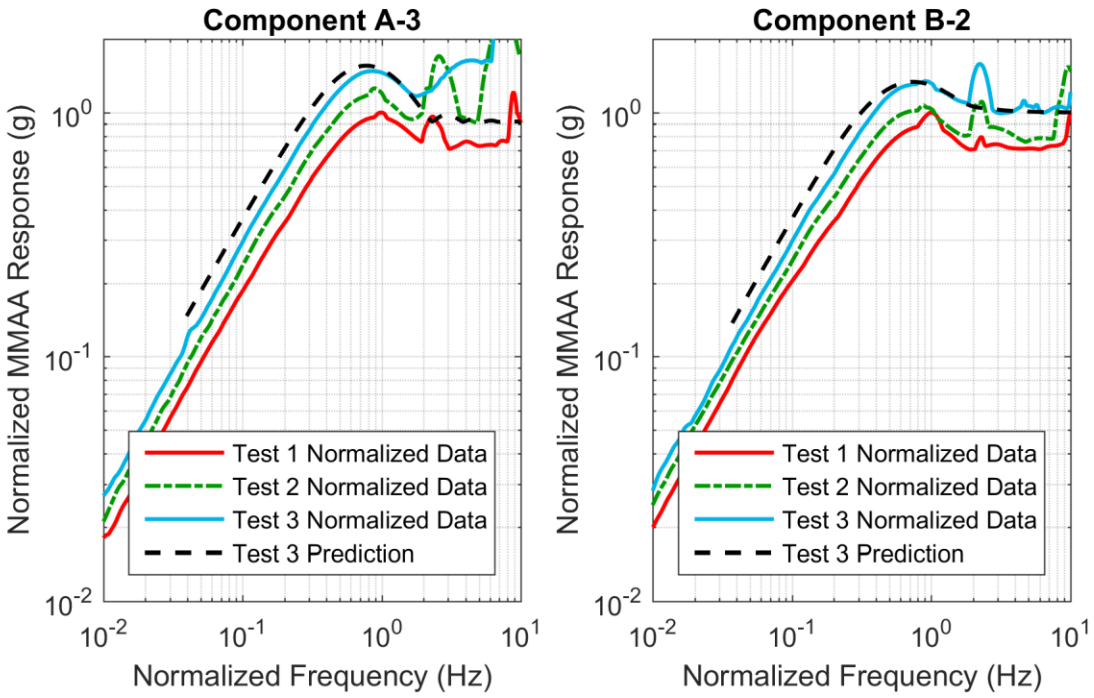

Figure 4. Sample Normalized Data from Tests 1, 2, and 3 Showing Shock Pulse SRS Shifting Along with the Test 3 Predictions from Theory

CONCLUSIONS

The conclusion from this investigation is that haversine scaling operation should always shift the SRS in both magnitude and pulse duration. The SRS shift should either result in a higher acceleration amplitude and a longer pulse duration or a lower acceleration amplitude and a shorter pulse duration. This allows for the extrapolation of haversine parameters based on drop height for future tests outside of the already tested envelope. The theoretical results can also be used to understand existing test data. Data that does not follow the scaling pattern described here likely indicates that a fundamental change in the system stiffness occurred during the test.

REFERENCES

1. Nelder, J. A. and Mead, R., "A Simplex Method for Function Minimization," *Computer Journal*, 1965, Vol. 7, pp. 308–313.